RSC Advances

ROYAL SOCIETY OF CHEMISTRY

www.rsc.org/advances

Journal Name

RSCPublishing

ARTICLE

Isothermal Crystallization Process of Poly (4-methyl-1-pentene)/Alkylated Graphene Oxide Nanocomposites: Thermal Analysis and Rheology Study

Cite this: DOI: 10.1039/xoxxoooooox

Received ooth January 2012,
Accepted ooth January 2012

DOI: 10.1039/xoxxoooooox

www.rsc.org/

Li-yang Xu, Bo Yin*, Huai-wen Yan, Ai-ping Ma, Ming-bo Yang*

In this work， alkylated graphene oxide (GO-ODA) was obtained successfully via electrostatic self-assembling of the oppositely charged GO and ODA. Then TPX/GO-ODA nanocomposites were obtained from solution method. And all samples have the same crystal structure, Form I, by X-ray diffraction (XRD). It was worth noting that the poly (4-methyl-1-pentene) (TPX) has two types of lamellae under the high crystallization temperature by differential scanning calorimetry (DSC). The higher crystallization temperature, the slower crystallization occurs, however, the nanofiller, GO-ODA, shows a great advantage in accelerating the crystallization. At the same time the added GO-ODA as nucleation improve the temperature of the Type II lamellae appearance. Moreover, crystal growing space is limited by the structure of GO-ODA. In rheological experiments, when the frequency was higher than a critical value, crystallization was no longer affected by the frequency. In this work, exploring such interplay between the crystallization behavior and crystallization rheology could guide to choose polymers in practical application and processing.

Introduction

Generally, highly transparent polymers are amorphous. But if the refraction index of the amorphous region is close to that of the crystalline region, the semi-crystalline polymers have a chance of being transparent materials. Poly(4-methyl-1-pentene) belongs to this category of highly transparent, crystalline polymers.[1] Poly (4-methyl-1-pentene) (PMP), trade name TPX, is an important industrial material because of its advantageous properties. These properties, especially the high melting temperature and the low density, are also intriguing from a scientific point of view. The high melting temperature corresponds to the significantly lower entropy of fusion of PMP compared with other polyolefin,[2, 3] and the lower entropy of fusion relates to the existence of an inhomogeneous structure in the melt.[2-4] PMP presents a complex polymorphic behavior, so five different crystalline forms have been reported. They can be obtained from crystallization in semidilute solutions depending on the solvent and the thermal history of the solutions.[5, 6] Form I is the most stable crystalline form, which packed in a tetragonal unit cell (a = 18.66 Å and c = 13.80 Å) with a 7/2 helical conformation according to the space group $P\bar{4}$. And the Form I can be obtained from the melt or from crystallization in high boiling solvents.[7, 8]

Graphene is a novel two-dimensional (2D) nanomaterial, a one-atom-thick sheet of sp2-hybridized carbon.[9] It can be viewed as molecular graphite or as an extralarge polycyclic aromatic molecule. It possesses several unique properties that are unseen in other materials, such as room-temperature quantum Hall effect, high mechanical strength, high elasticity and thermal conductivity, and tunable bandgap. However, some approaches[9-12] to synthesize the pure graphene has a certain difficulty, we prepared graphene through chemical synthesis (Improved Hummers' method[13]). And the product (GO) obtained by this method can be retained the original structure of grapheme,[14] however, it has a great deal of epoxy, hydroxyl and carboxyl functional groups on the single layer structure, which determined the GO polar. Followed, we can change the nucleation ability of GO via the electrostatic assembling method to have a homogeneous dispersion in the PMP.

It is well known to all that many researches have focused on the crystallization kinetics with rheological measurements to detect the shear influence on crystallization.[15, 16] As far as we know, however, there are only a few reports[17] focusing on this issue as it is difficult to get a stable liquid-solid state of polymer melt when studying the influence of crystallites on the rheological properties of the melt at a given degree of crystallinity.[18, 19] Winter et al.[20, 21] has reported that they explore routes to get stable critical gel, where the semicrystalline structure is stable

and the crystallinity is sufficiently low. And the critical gel was found to be relatively soft, having a surprisingly high relaxation exponent. The literature[18, 19] has reported that measuring the rheological properties of semicrystalline polymer with a given degree of crystallization at a condition where the crystallinity of the system is steady for a relatively long time, thus allowing reliable and reproducible measurements. And Grizzuti et al. propose a novel method, "inverse quenching", to get such conditions and use it to measure the rheological properties of polymer. M.R. Nobile et al.[22] have studied that the isothermal crystallization of i-PP with rheological technique. They choose a suitable crystallization temperature by quiescent crystallization experiments to study the flow effect. And with analysis, they found that the recovery of the molecular orientation induced by the shear flow did not occur above the critical shear rate value. In the extrusion or injection molding, PMP is processed into products going through the change from melt to crystallization, resulting that crystal lattice is always the tetragonal lattice that exhibits interlocking. Therefore, to control the properties of PMP, it is important to understand and control the higher order structures in its hierarchy. Up to now, almost no literature reports the crystallization rheological properties of PMP and their composites. Our purpose is to report the rheological characterization of PMP and composites. Rheological behaviour change is used to record the crystallization process of the semi-crystalline PMP samples. Exploring such interplay between the crystallization behavior and crystallization rheology could not only guide to choose polymers in practical application and processing but will also lead to a general methodology applicable for all traditional semi-crystalline polymers.

Experimental

Materials

In this paper, the poly (4-methyl-1-pentene) (trade name TPX), was purchased from Mitsui Chemicals Americal, Inc. The solvent was chemically pure (99.5%) cyclohexane and was used without further purification. The graphite flake was got from Research Institute of Shenghua, Changsha, Hunan, China.

Sample preparation

The modifed graphene (GO-ODA, the octadecylamine grafted to GO) was got according to the methods the previous paper mentioned.[23] Then two types of samples were obtained with the same method: TPX and TPX/GO-ODA (0.5 wt%).

The prepared samples were also dried at 60 ^{o}C for 72 h and then compression molded into disks with the diameter of 25 mm and the thickness of 1 mm on a hot-stage at 250 ^{o}C and cooled on a cold-stage at room temperature under the pressure of 10 MPa, which were used for the rheological tests and DSC tests.

XRD characterization

All samples were characterized by a DX-1000 automatic X-ray diffractometer with CuKα radiation (λ = 1.54 Å) at a generator voltage of 40 kV and a generator current of 40 mA operating at a step size of 0.02 ° from 5 ^{o} to 40 ^{o}.

DSC Characterization

The crystallization behaviors of samples were measured with a TA DSC Q20 (TA Instruments, USA). About 5 to 10 mg of each sample was encapsulated in aluminum pans and heated up to 260 ^{o}C for 2 min and cooled to different crystallization temperature, 218-230 ^{o}C for 60 min. Then the melt were cooled to 100 ^{o}C with a cooling rate of 50 ^{o}C•min^{-1}; the second heating were set to 260 ^{o}C with a heating rate of 10 ^{o}C•min^{-1} to study the melting behavior. The melting transition temperature (T_m) was determined as the maximum of the corresponding transition peaks. All measurements were carried out in a nitrogen atmosphere with an intercooler connected to keep stable control.

Rheological characterization

As mentioned previously papers, different authors[15, 24] had used the dynamic rheological measurements to study the crystallization. In this type of experiment, the disturbance of crystallization caused by the shear and strain must be taken into account. However, the dimensional variation of the sample during the crystallization was often neglected though it may induce large errors on the measurements due to additional stress on the sample and uncertainties in the calculation.

The oscillatory shear measurements were carried out on stress controlled dynamic rheometer AR2000ex (TA, USA) equipped with 25 mm parallel plates. All measurements were performed under the protection of nitrogen atmosphere. During the measurements, the sample and plates were enclosed in a high temperature chamber and heated. The samples about 1mm in thickness were melted at 260 ^{o}C for 2 min in the parallel-plate fixture to erase any memory of previous structure. After that, the sample was cooled to the crystallizing temperature at 7 ^{o}C•min^{-1} by nitrogen convection. Each test requires thermal equilibration at crystallizing temperature in 1 min. Our tests were at crystallizing temperature, 224 ^{o}C, with the frequencies of 0.1, 1, 10, 100 Hz, respectively. And measurements were at the same frequency, 1 Hz, with different crystallizing temperature, 226 ^{o}C, 228 ^{o}C, 230 ^{o}C.

Results and discussion

X-ray photoelectron spectrometer (XPS) and Fourier-transform infrared spectrometer (FTIR) had been used to test the GO-ODA，it is sure that the ODA grafted to GO successfully.[23]

X-ray diffraction is a powerful tool to characterize semi-crystalline polymers. To further demonstrate the crystal structure of TPX, XRD spectra of samples was shown in Figure 1. It is observed that the diffraction peaks location of TPX/GO-ODA (0.5 wt%) and TPX are coincident, and the GO-ODA has no effect on the XRD patterns of nanocomposites. In the present reports the TPX has five crystalline modifications with X-ray diffraction profiles, the crystal structure our samples are Form I.

Isothermal crystallization under quiescent conditions

For all the samples, the crystallization process prolongs with increasing crystallization temperature. Figure 2 shows the typical heat flow curves of samples during isothermal crystallization at different crystallization temperature and DSC melting traces of TPX and TPX/GO-ODA isothermally crystallized at different temperatures is embedded respectively. Compared with 218 ^{o}C, the higher crystallization temperature, the longer time for crystallization; however, TPX/GO-ODA (0.5 wt%) at all crystallization temperature show relatively lower peak time values and narrower peak time ranges, which indicates that the crystallization rates of TPX/GO-ODA(0.5 wt%) are faster than that of TPX. At high temperature, the crystallization rate is slow that is limited by the temperature. However, like other nanofiller, the added GO-ODA is also nucleation point, which increases the amount of nucleation point and accelerates crystallization. Moreover, crystal growing space is limited by the structure of GO-ODA. In the previous reports, C. Sivestre[25] and Bassett et al[26] found that two melting peaks of samples are related with lamellae thicknesses that formed in two stages of crystallization. In our work, we also find the same phenomenon that was in agreement with literatures. The peaks around 220 ^{o}C, Type II lamellae,[25] become more clearly with the crystallization temperature increasing to 228 ^{o}C and the peaks around 236 ^{o}C are stable. It is obvious that the Type II lamellae growth of samples is related to temperature, and the Type I regularity is depend on crystallization temperature. Then the samples melting enthalpy and melting temperature (T_m) are shown in Figure 3. It is obvious that the differences of samples melting enthalpy values at different crystallization temperature are around 30 J•g^{-1} and TPX/GO-ODA (0.5 wt%) values are relatively smaller than TPX. However, as the crystallization temperature increasing, the melting temperature of TPX and TPX/GO-ODA (0.5 wt%) are increased respectively, except T_c = 230 ^{o}C. The reason for this phenomenon is that the arrangement regularity increase with crystallization temperature increasing leading to melting entropy reduced, then the melting temperature of samples increased according to thermodynamic equilibrium. But when the crystallization temperature of TPX is 228 ^{o}C, Type I lamellae could grow surround Type II lamellae, so the melting peak is broad as shown in Figure 2a (inserted). The formation of Type II lamellae is related with not only the higher undercooling, but also as a consequence of the difficulties of the lamellae to accommodate to the environment of previously formed lamellae. And this phenomenon of TPX/GO-ODA is emerge at 230 ^{o}C, the reason is that GO-ODA makes the lamellae spatial growth reduced and hinders the growth of two types lamellae. As we all known that the added nanofiller is equivalent to nucleation points, however, it also limit the growth spatial of lamellae because of the Type II lamellae of TPX/GO-ODA (0.5 wt%) occurs later than that of TPX. This phenomenon is shown in Figure 4. When temperature increasing, the Type I lamellae grow surround Type II lamellae, the regularity increases with temperature increasing and the amount of Type II lamellae is small, so the melting peaks of Type I lamellae is higher. And the arrangement of Type I and Type II lamellae is close at high crystallization temperature, so the melting peaks are broad.

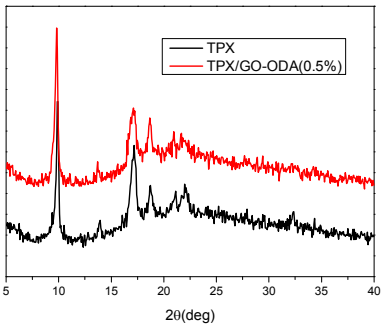

Figure 1. The X-ray diffraction pattern of TPX and TPX/GO-ODA(0.5 wt%).

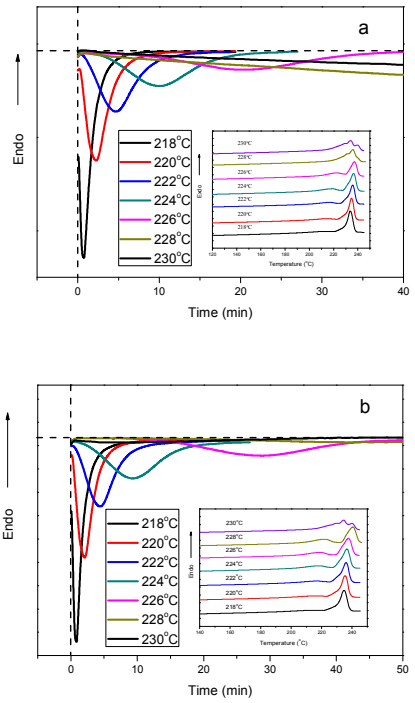

Figure 2. DSC heat flow curves during isothermal crystallization at different crystallization temperature for (a), TPX; (b), TPX/GO-ODA (0.5 wt%). Inset shows melting traces of samples after Isothermal crystallization.

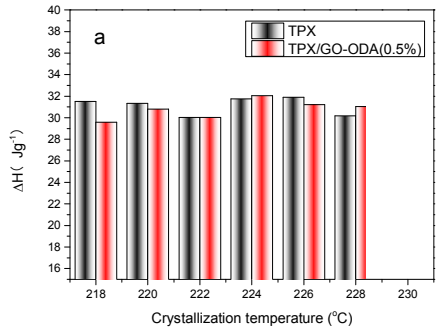

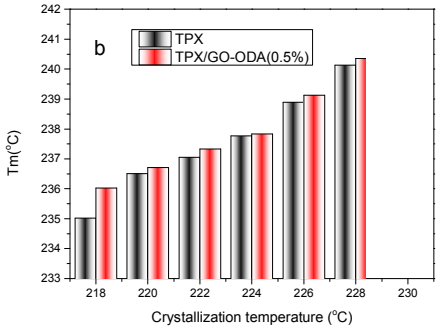

Figure 3. Melting enthalpy (a) and melting temperature (b) of TPX and TPX/GO-ODA (0.5 wt%) after isothermal crystallization at different temperature.

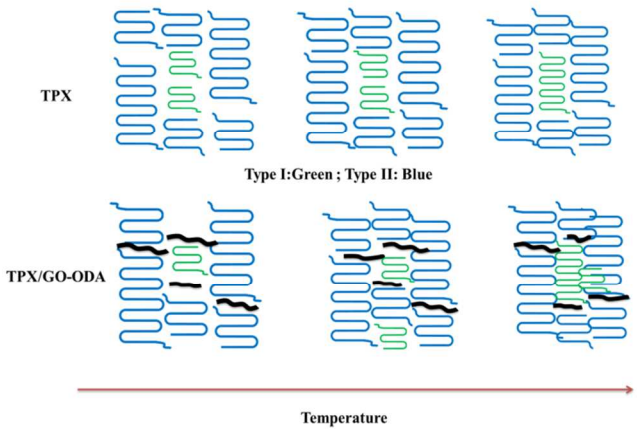

Figure 4. The schematic diagram of lamellae arrangement under different temperatures.

Isothermal crystallization under shear

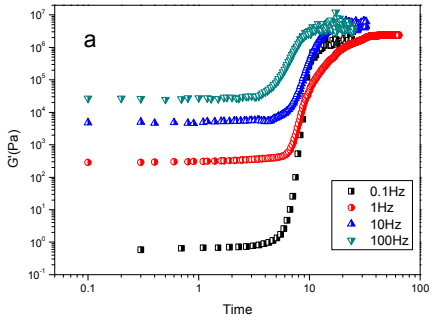

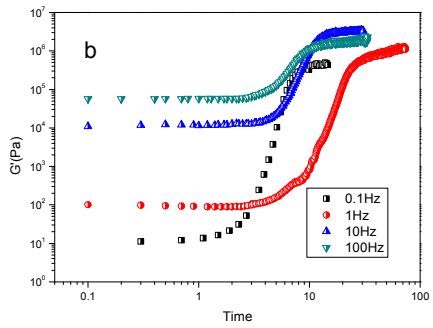

Figure 5. The evolution of storage modulus with time during the isothermal crystallization of sample at 224 °C with different frequencies: a,TPX; b, TPX/GO-ODA(0.5%).

For TPX and TPX/GO-ODA composites, developments of storage modulus (G') during dynamic shear under different frequency at crystallization temperatures 224 °C are shown in Figure 5. To control the crystallization speed, a suitable crystallization temperature, 224 °C, is chose to test and observe in the experimental results with the rheometer. Figure 5 shows storage modulus G' with TPX and TPX/GO-ODA (0.5 wt%). During the test, there is no significant deviation from a sinusoidal stress signal. During the 224 °C isothermal measurements, the rheological structure of the TPX and TPX/GO-ODA (0.5 wt%) varies from the amorphous state to crystalline state. In the early experiments, the G' are constant values before the crystallization starting. As crystallization developed, the upturn time at which G' increase quickly, then the G' approach the plateau values at the end of the primary crystallization stage. In other word, the function of storage modulus, G', and time shows a sigmoidal shape. It is obvious that storage modulus, G', increase with increasing frequency in the early and the upturn time of the TPX is longer than TPX/GO-ODA (0.5 wt%) at different frequency. It is clearly that the reason for the plateau values for G' at the end of the primary crystallization stage have some fluctuations is that the slight differences between the parallel plates of rheometer in the sample position and the fluctuations in the gap distance, thus the two aspects will affect the response of samples.[27]

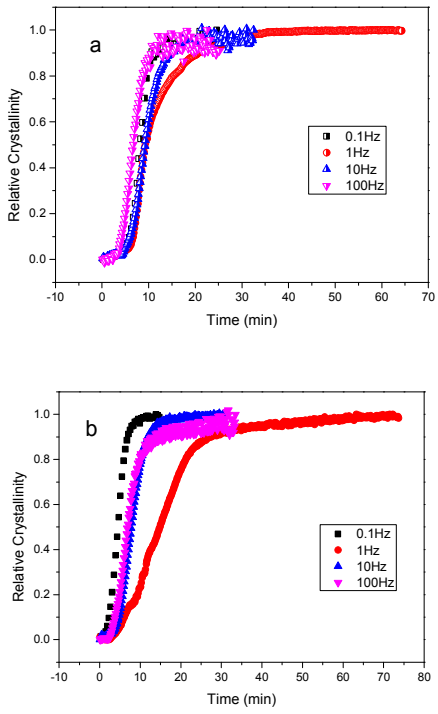

Figure 6. Changes of relative crystallinity, x(t), with time during crystallization at 224 °C for (a) TPX and (b) TPX/GO-ODA with different frequencies.

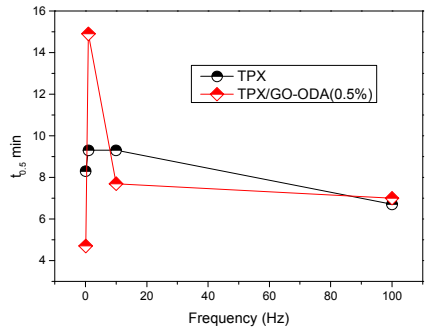

Figure 7. Changes of crystallization half time, $t_{1/2}$, with frequency for TPX and TPX/GO-ODA(0.5 wt%) at T_c = 224 °C.

Although the above dynamic mechanical spectroscopy provides a reliable tool to probe different aspects of the (flow induced) crystallization process, such as a relative level of crystallinity and timescales of the evolution, the mechanical data is not so simple.[28] However, Pogodina et al. have proposed that a logarithmic normalization of the G' data is used to applying for an estimation of the transformed fraction as follow.[29]

$$X_{(t)} = \frac{\log G'_{(t)} - \log G'_{\min}}{\log G'_{\max} - \log G'_{\min}}$$

Where G'_{min} and G'_{max} are the values of the starting storage modulus and ending plateau storage modulus, respectively. The frequency effect on the isothermal crystallization of TPX and TPX/GO-ODA (0.5 wt%) is analyzed by defining the crystallization half time, $t_{1/2}$, at which half of the change in the viscoelastic functions occurs. The changes of relative crystallinity with time during crystallization at T_c = 224 °C for samples under the quiescent condition are shown in Figure 6. This figure shows that the presence of GO-ODA in the composites causes the onset of crystallization to occur earlier in most frequency. The influences of frequency on the crystallization half time, $t_{1/2}$, are shown in Figure 7. It can be clearly seen that the changes of crystallization half time for TPX can not get an accurate conclsion. But for TPX/GO-ODA (0.5 wt%), the crystallization half time has a great change in the low frequency region. And the crystallization half time with frequency tends to be a line that parallel to abscissa in the high frequency region. At the same time, the crystallization half time of TPX and TPX/GO-ODA (0.5 wt%) is almost uniform. Regularity under dynamic rheological condition has a certain trend, which may have a reference value during crystallization process under actual external field.

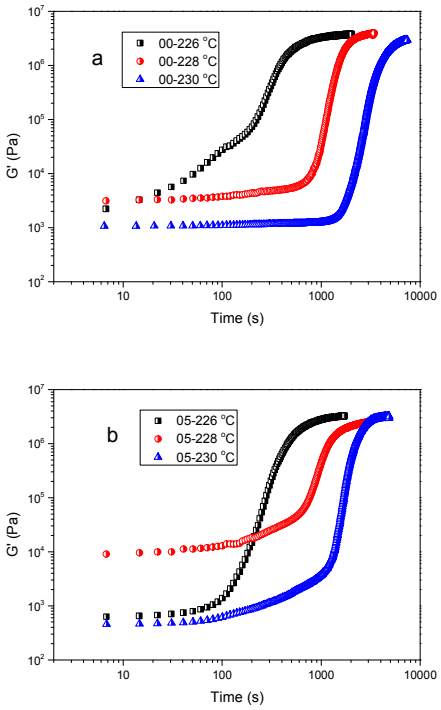

Figure 8. The evolution of the storage modulus with time for the different Temperature (a) TPX ; (b) TPX/GO-ODA(0.5 wt%).

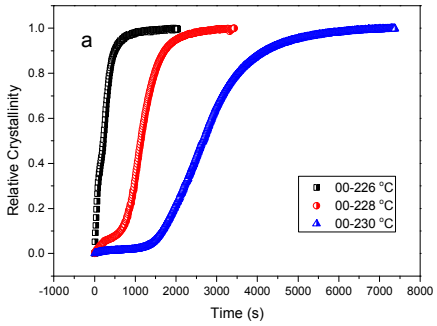

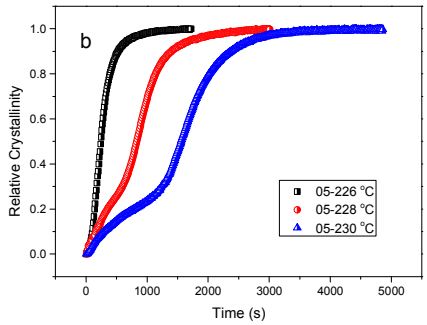

Figure 9. Changes of relative crystallinity, with time during crystallization at diffrnent crystallization temperature for (a) TPX and (b) TPX/GO-ODA(0.5 wt%).

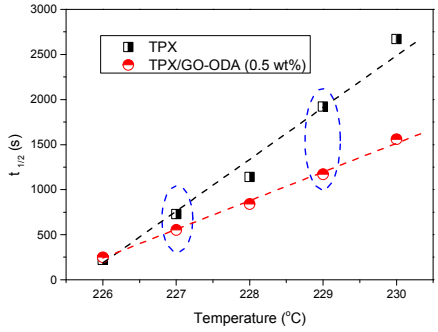

Figure 10. Changes of crystallization half time, $t_{1/2}$, with crystallization temperature for TPX and TPX/GO-ODA (0.5 wt%).

The evolution of the storage modulus for both neat TPX and the TPX/GO-ODA (0.5 wt%) nanocomposites samples at different crystallization temperatures are shown in Figure 8. The change of each sample storage modulus, G', with time shows a sigmoidal shape. The evolution of the kinetics process (the slope of the curves) is affected by the crystallization temperature in the TPX, a gradual change in the process is observed in Figure 6a. Such changes are same for TPX/GO-ODA (0.5 wt%) (Figure 8b). Then according to the equation (1), we get Figure 9, which demonstrates the changes of relative crystallinity with time during different crystallization temperature for samples. At last, the changes of crystallization half time with crystallization temperature are shown in Figure 10. The dotted lines indicate the trend variation and the data in the dotted ellipses are evaluated. It is worth noting that the crystallization half time increases with the crystallization temperature increasing for TPX and TPX/GO-ODA (0.5 wt%). At the same time the crystallization half time of TPX/GO-ODA (0.5 wt%) is shorter than that of TPX, which suggests that GO-ODA could accelerate crystallization. But temperature is the major factor for crystallization at 226 °C, when crystallization temperature is higher, GO-ODA will play a role of accelerating the crystallization.

From the physical point of view, the basic mechanisms which lead to flow-induced crystallization are relatively well understood. When flow is applied to polymer melt, the conformational change depending on the type and intensity of the flow field takes place and produces alignment and possible stretching of the chains. Polymer chains in this perturbed, more ordered conformational state, possess a higher free energy, which thus increases the driving force for the crystallization process, and the relative kinetics become faster. As to polymer melts, the ability of flow to produce conformational changes with respect to the equilibrium, isotropic state, results from the coupling between the flow intensity and the relaxation behavior of the polymer chains.[30, 31]

In this case, the TPX and TPX/GO-ODA (0.5 wt%) have no distinct effects on the rheological responses of the melt. All samples have low storage modulus at the beginning of crystallization, which is due to the fact that most chains are amorphous and chains are random state. With the time increasing, the crystallization occurs slowly and the chains form an orderly arrangement gradually. So storage modulus increase and approach the plateau values because of rigidity increasing. And the arrangement of molecular chains is also shown in Figure 4. The evolution of storage modulus increases with time during the isothermal crystallization of sample at different frequency, which is due to the shorter response time of molecules. In our case, the frequency has a great impact on the molecular chain arrangement. In low-frequency region, the crystallization half time grows with frequency increased; in high-frequency region, the crystallization half time will be a constant value with frequency increased. It is obvious that frequency has a critical value where the crystallization rate will no longer be affected by frequency. The influence of crystallization temperature on the crystallization rate is consistent with the DSC results. And the lamellae growth has been descripted in this part. Temperature and nanofiller are important factors for isothermal crystallization, where the higher crystallization temperature, the slower crystallization occurs, however, the nanofiller, GO-ODA, shows a great advantage in accelerating the crystallization. At high temperature, the crystallization rate is slow that is limited by the temperature. However, like other nanofiller, the added GO-ODA is also nucleation point, which increases the amount of nucleation point and accelerates crystallization. Moreover, crystal growing space is limited by the structure of GO-ODA.

Conclusions

In this work， GO-ODA was obtained successfully via electrostatic self-assembling of the oppositely charged GO and ODA. And all samples have the same crystal structure by XRD. Temperature and nanofiller are important factors for isothermal crystallization, where the higher crystallization temperature, the slower crystallization occurs, however, the nanofiller, GO-ODA, shows a great advantage in accelerating the crystallization. The added GO-ODA is nucleation point, which increases the amount of nucleation point and accelerates crystallization. Moreover, crystal growing space is limited by the structure of GO-ODA. But it is found that the TPX has two types of lamellae in the high crystallization temperature. And the emergence of Type II lamellae melting peak is related to crystallization temperature and the added GO-ODA improves the temperature of the Type II lamellae appearance. In rheological experiments, the effects of temperature on the crystallization rate are consistent with the DSC results. And the influence of frequency on crystallization rate, the frequency has a critical value, and when the frequency is higher than that, crystallization is no longer affected by the frequency. At the same time the nanofiller, GO-ODA, show a great advantage in accelerating the crystallization. In this work, exploring such interplay between the crystallization behavior and rheological characteristics will not only provide an important guide in the choice of these polymers for application and in processing

design but will also lead to a general methodology applicable to all traditional semi-crystalline polymers.

Acknowledgements

The authors gratefully acknowledge the financial support from the National Natural Science Foundation of China (Contract No. 51273219 and 5142106), the National Key Basic Research Program of China (973 Program, No. 2012CB025902), the Foundation of State Key Laboratory of Polymer Materials Engineering (Grant No. sklpme2014-3-12) and the Fundamental Research Funds for the Central Universities (No. 2013SCU04A03).

Notes and references

College of Polymer Science and Engineering, State Key Laboratory of Polymer Materials Engineering, Sichuan University, Chengdu, 610065 Sichuan, China. Fax:+86-28-8540-5324 Tel:+86-028-8540-5324 E-mail: yinbo@scu.edu.cn; Fax: +86-028-8540-5234; Tel: +86-028-8540-1988 E-mail: yangmb@scu.edu.cn

1 Kissin, Y. Wiley-Interscience, Encyclopedia of Polymer Science and Engineering. 1987, 9, 707-718.
2. Wilkes, C. E.; Lehr, M. H. Journal of Macromolecular Science, Part B: Physics 1973, 7, (2), 225-230.
3. Mita, K.; Okumura, H.; Kimura, K.; Isaki, T.; Takenaka, M.; Kanaya, T. Polymer Journal 2012, 45, (1), 79-86.
4. Pratt, C.; Geil, P. Journal of Macromolecular Science, Part B: Physics 1982, 21, (4), 617-649.
5. Charlet, G.; Delmas, G. Polymer 1984, 25, (11), 1619-1625.
6. Charlet, G.; Delmas, G.; Revol, J.; Manley, R. S. J. Polymer 1984, 25, (11), 1613-1618.
7. Kusanagi, H.; Takase, M.; Chatani, Y.; Tadokoro, H. Journal of Polymer Science: Polymer Physics Edition 1978, 16, (1), 131-142.
8. Bassi, I.; Bonsignori, O.; Lorenzi, G.; Pino, P.; Corradini, P.; Temussi, P. Journal of Polymer Science Part A - 2: Polymer Physics 1971, 9, (2), 193-208.
9. Novoselov, K. S.; Geim, A. K.; Morozov, S.; Jiang, D.; Zhang, Y.; Dubonos, S.; Grigorieva, I.; Firsov, A. Science 2004, 306, (5696), 666-669.
10. Novoselov, K.; Geim, A. K.; Morozov, S.; Jiang, D.; Katsnelson, M.; Grigorieva, I.; Dubonos, S.; Firsov, A. nature 2005, 438, (7065), 197-200.
11. Berger, C.; Song, Z.; Li, X.; Wu, X.; Brown, N.; Naud, C.; Mayou, D.; Li, T.; Hass, J.; Marchenkov, A. N. Science 2006, 312, (5777), 1191-1196.
12. Li, X.; Cai, W.; An, J.; Kim, S.; Nah, J.; Yang, D.; Piner, R.; Velamakanni, A.; Jung, I.; Tutuc, E. Science 2009, 324, (5932), 1312-1314.
13. Marcano, D. C.; Kosynkin, D. V.; Berlin, J. M.; Sinitskii, A.; Sun, Z.; Slesarev, A.; Alemany, L. B.; Lu, W.; Tour, J. M. ACS nano 2010, 4, (8), 4806-4814.
14. Park, S.; Ruoff, R. S. Nature nanotechnology 2009, 4, (4), 217-224.
15. Teh, J.; Blom, H.; Rudin, A. Polymer 1994, 35, (8), 1680-1687.
16. Masubuchi, Y.; Watanabe, K.; Nagatake, W.; Takimoto, J.-I.; Koyama, K. Polymer 2001, 42, (11), 5023-5027.
17. Watanabe, K.; Okada, K.; Toda, A.; Yamazaki, S.; Taniguchi, T.; Koyama, K.; Yamada, K.; Hikosaka, M. Macromolecules 2006, 39, (4), 1515-1524.
18. Coppola, S.; Acierno, S.; Grizzuti, N.; Vlassopoulos, D. Macromolecules 2006, 39, (4), 1507-1514.
19. Acierno, S.; Grizzuti, N. Journal of Rheology (1978-present) 2003, 47, (2), 563-576.
20. Pogodina, N. V.; Lavrenko, V. P.; Srinivas, S.; Winter, H. H. Polymer 2001, 42, (21), 9031-9043.
21. Horst, R. H.; Winter, H. H. Macromolecules 2000, 33, (20), 7538-7543.
22. Nobile, M.; Bove, L.; Somma, E.; Kruszelnicka, I.; Sterzynski, T. Polymer Engineering & Science 2005, 45, (2), 153-162.
23. Xu, L.-y.; Yan, H.-w.; Gong, L.; Yin, B.; Yang, M.-b. RSC Advances 2015, 5, (6), 4238-4244.
24. Te Nijenhuis, K.; Winter, H. H. Macromolecules 1989, 22, (1), 411-414.
25. Silvestre, C.; Cimmino, S.; Di Pace, E.; Di Lorenzo, M. L.; Orsello, G.; Karasz, F. E.; Lin, J. S. J. Mater. Sci. 2001, 36, (12), 2865-2874.
26. Bassett, D.; Patel, D. Polymer 1994, 35, (9), 1855-1862.
27. Zhong, Y.; Fang, H.; Zhang, Y.; Wang, Z.; Yang, J.; Wang, Z. ACS Sustainable Chemistry & Engineering 2013, 1, (6), 663-672.
28. Vega, J. F.; Hristova, D. G.; Peters, G. W. J. Therm. Anal. Calorim. 2009, 98, (3), 655-666.
29. Pogodina, N. V.; Winter, H. H.; Srinivas, S. Journal of Polymer Science Part B Polymer Physics 1999, 37, (24), 3512-3519.
30. Coppola, S.; Grizzuti, N.; Maffettone, P. L. Macromolecules 2001, 34, (14), 5030-5036.
31. Acierno, S.; Palomba, B.; Winter, H. H.; Grizzuti, N. Rheologica acta 2003, 42, (3), 243-250.